Global NEST Journal, Vol 25, No 5, pp 28-33

Performance, material degradation and durability of an ammonia chemical scrubber operated under acidic conditions

Psarras S.[1,*], Pegkos D.[1], Dimoka P.[1], Eftaxias A.[2], Charitidis P.[2], Diamantis V.[2] and Kostopoulos V.[1]
[1]Department of Mechanical Engineering and Aeronautics, University of Patras, GR26500, Patras, Greece.
[2]Department of Environmental Engineering, Democritus University of Thrace, GR67100 Xanthi, Greece.
Received: 03/07/2022, Accepted: 01/11/2022, Available online: 31/01/2023
*to whom all correspondence should be addressed: e-mail: spsarras@upatras.gr
https://doi.org/10.30955/gnj.004394

Graphical abstract

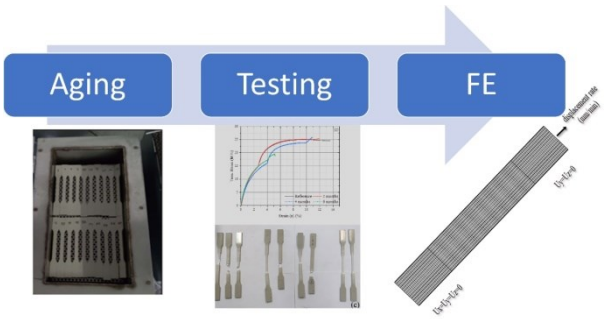

Abstract

The aim of this study was to investigate the tensile strength reduction of four different materials: steel, polypropylene, polyethylene and glass fiber/epoxy (GFRP), under the conditions in a chemical scrubber. . For this reason a pilot-scale scrubber was operated at influent ammonia concentrations between 4000-4200 ppm with gradually decreasing pH. Optimum process performance was achieved at low pH=2.0 and this scrubber liquid used to study the aging of different construction materials, over a six month period.. The outcomes of the study revealed that thermoplastic materials and especially polypropylene are suitable for biogas applications under acidic conditions as their strength and modulus of elasticity remained highly unaffected. For steel specimens, the experimental results showed that failure was due to propagation of a single crack, while the failure of GFRP was caused by multiple microcracks (defects and voids) in the matrix. Finally, the data generated were capable to predict the aging effect on the strength when used to finite element simulations.

Keywords: Ammonia absorption, chemical scrubber, thermoplastic, glass fibers, finite element method

1. Introduction

Anaerobic digestion is a biochemical process used for the conversion of organic compounds to methane-rich biogas (Diamantis *et al.*, 2021). Simultaneously, ammonia is generated by the anaerobic degradation of proteins, which remain mostly in the liquid phase under the pH conditions prevailing in anaerobic digestion facilities (pH 7.0-8.0). Ammonia is an essential element for the growth of methanogenic bacteria but also an inhibition factor, when present at high concentrations (> 3 g/L) (Spyridonidis *et al.*, 2022). The digestate, on the other hand, is used as an organic soil conditioner since both organic and inorganic compounds (macro- and micro-nutrients) are present at variable concentrations (EU Regulation, 2019).

Ammonia removal from the anaerobic digester effluent is possible by implementing a chemical stripping process (Georgiou *et al.*, 2019). The latter method utilizes air to strip the ammonia present in the liquid phase to the gaseous phase under alkaline conditions. Recently, Matassa et al (Matassa *et al.*, 2022) demonstrated that it was possible to strip ammonia from an anaerobic digester effluent by 40-50% using air, without the addition of alkaline reagents. The ammonia recovered in the gaseous phase can thus be concentrated by chemical absorption. The latter method is often performed by the addition of acidic reagents such as sulfuric acid.

Corrosion management and prevention is a critical factor in many industrial settings (Roberge, 2008). Sometimes corrosion can cause serious consequences in the environment (Landolt, 1993). It was reported that more than 25% of the total economic losses in the oil and gas (and biogas) industry are due to failures of pipes and other plant components resulting from metallic corrosion (Durnie *et al.*, 1999; Bentiss *et al.*, 2000; Sastri, 1998). This problem is usually overcome by using high density polyethylene (e.g. carbon steel pipes) which have a good corrosion resistance and low cost (Samimi and Zarinabadi, 2011; Samimi and Zarinabadi, 2012; Tallman *et al.*, 1999). Thermoplastic materials such as polyethylene (PE) and polypropylene (PP) do not rust like metal and thus can be used in applications where rust would be a problem (Miao *et al.*, 2018; Qi *et al.*, 2011; Mano *et al.*, 2001; Azuma *et al.*, 2009). Further on, glass fiber reinforced polymer (GFRP) provide resistance to environmental solutions as well as excellent strength and stiffness to weight ratios (Robert and Benmokrane, 2013; Al-Salloum *et al.*, 2013; Chen *et al.*, 2007; Liao *et al.*, 1999). There exists a considerable body of

literature on thermoplastic materials and polymeric composites. Many of them analyzed their mechanical performance only when exposed to aggressive environments (Han and Nairn, 2003; Bergeret and Ienny, 2009; Haddar*et al.*, 2014; Karger-Kocsis, 1991; Kawaia *et al.*, 2017; Barbouchi *et al.*, 2007; Sindhu *et al.*, 2007; Kim and Youn, 2007). Their results shown that mechanical properties such as tensile strength and modulus of elasticity will be increased in acid environment and decrease for other kind of solvents.

Aim of this study was to evaluate the performance of a chemical scrubber to remove ammonia from air under different pH conditions. Optimum pH conditions were thus identified and scrubber liquid was used to study the aging of different construction materials. The latter included steel, polypropylene, polyethylene and GFRP. The strength and durability were studied over a six month period using tensile standard tests in order to evaluate the strength reduction. The outcomes of the test campaign were used as input to Finite Element (FE) models and comparisons were made.

2. Materials and Methods

2.1. Chemical scrubber design and operation

Ammonia absorption was studied using a scrubber packed with pall rings. The scrubber was 150 cm in height and 5 cm in diameter. The system was operated with ambient air having ammonia concentrations between 4000-4200 ppm, similar to those recovered during air stripping of anaerobic digester effluent (Georgiou *et al.*, 2019). The air flowrate to the absorber column was maintained between 150 and 1500 L/h. The operational temperature varied between 25 and 30 ^{o}C while the absorber pH increased from 1.0 to 2.0, 5.5, 6.5 and 7.5. Process efficiency was evaluated based on the influent and effluent NH_3 concentration using draeger tubes (Draeger, Germany).

2.2. Materials and specimens' preparation

Materials such as steel (St-37), polyethylene (PE), polypropylene (PP) and glass fiber reinforced polymer (GFRP) were investigated in this study. A total of 112 specimens (7 specimens for each case) were manufactured and tested. Polyethylene (PE-100) and polypropylene (PP) sheets were provided by Stemplast company (Greece) while steel plates (St-37) were supplied by Chryssafidis company (Greece). The GFRP specimens had an average thickness of 2.3mm (12 layers of 0o). The composite material was thawed, unrolled, and cut into the desired sizes. Further on the composite was cured at 1 bar and 120 oC for 1 hour under pressure and vacuum to produce hardened composite plates.

2.3. Specimen configuration

The testing configurations were based on ASTM standards; EN 527.04 for GFRP, EN 527.02-03 for thermoplastic materials and EN 6892 for steel St-37. The specimen dimensions per type of material are shown in Figure 1.

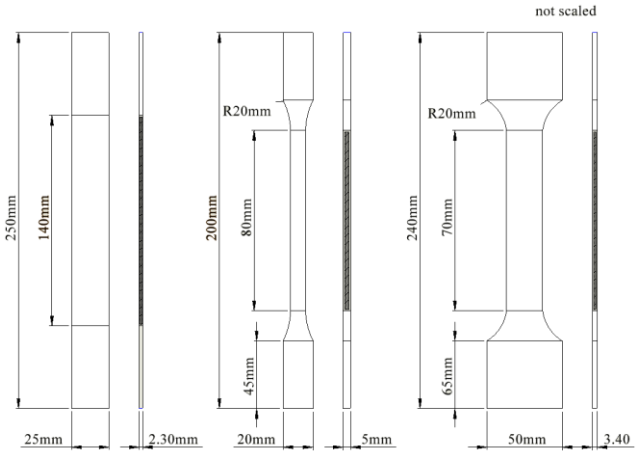

Figure 1. Dimensions of specimens of (a) GFRP (EN 527.04), (b) thermoplastic materials (EN 527.02) and (c) steel St-37 (EN 6892).

2.4. Hygrothermal conditions

Specimens were completely immersed in a metal bath containing an acidic scrubber solution with pH 2.0 at a constant temperature of 24^{o}C for the entire period of the experiments (6 months) simulating the environment of the chemical scrubber used for ammonia absorption (Figure 2).

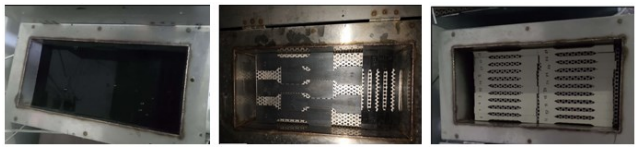

Figure 2. Direct immersed of specimens in metal bath containing acidic scrubber solution.

Hydration is the main cause of material degradation of steel materials. However, it must be mentioned that residual stresses are generated during the injection moulding process to produce polymer components. These residual stresses when combined with aggressive liquid media can cause unexpected brittle failure (environmental stress cracking) (Postawa and Kwiatkowski, 2006; Chen *et al.*, 2000; Zhou and Li, 2005; Pons *et al.*, 2011; Bowden and Young, 1974). The durability of specimens will determine the safety of the structures.

2.5. Mechanical testing

Tensile tests were performed on two different Universal testing machines. Instron 8872 and Instron 8802 at a speed of 1mm/min according to EN 527.04 for GFRP, EN 527.02-03 for thermoplastic materials and EN 6892 for steel St-37. The strain of the specimens was measured with the Instron extensometer in all tests as in Figure 3. Due to the large strain at failure at the metals, where the extensometer did not allow us to measure it (max elogation 5mm), they were marked before each test, on the free length of the specimen, and then the resulting elongation was measured. This technique was only used for this measurement: strain at break.

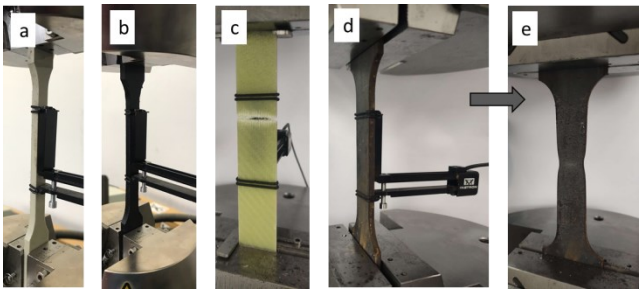

Figure 3. Testing configuration of specimens according to min according to (a) EN 527.04 for GFRP, (b-c) EN 527.02-03 for thermoplastic materials and (d-e) EN 6892 for steel St-37.

All tests were conducted at room temperature, while specimens were tested up to failure. For each case, seven (7) repeat specimens were summarized for the average stress–strain curve. The average values of the immersed specimens will be compared with the corresponding reference specimen (unsoaked specimen).

3. Results and discussion

3.1. Chemical scrubber performance

The pilot-scale scrubber was operated with gradually decreasing pH which was accomplished by dosing sulfuric acid via the pH control system. The experimental results, Figure 4, showed that with decreasing absorber pH ammonia concentrations at the effluent decreased significantly. Considering the above it was obvious that optimum ammonia removal is achieved at low pH and this value (2.0) was selected for the aging experiments.

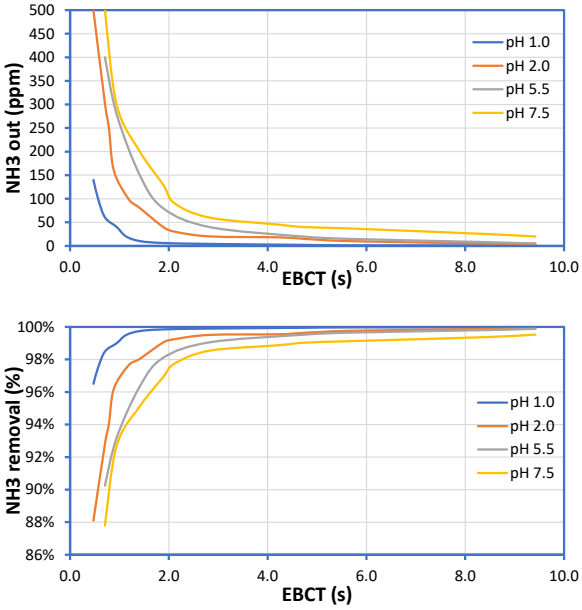

Figure 4 Effect of pH and empty bed contact time on (a) effluent ammonia concentration and (b) ammonia removal efficiency, during absorber operation.

3.2. Material degradation and durability

The behavior of the specimens was monitored, and the tensile strength and modulus of elasticity were studied at pH values 2.0. Figures 5a-d show the tensile stress and strain curves of the specimens. They demonstrate that the tensile strength decreases with the increase of exposure time. Furthermore, there was a linear increase of the load with the displacement, followed by a nonlinear behaviour. Young's Modulus of the specimens was predicted when the maximum load was obtained Figures 5a-c. For thermoplastic specimens, a shear banding phenomenon has been observed just before the yield point (Lüders bands) (Detrez and Roland, 2008; Drozdov and Christiansen, 2003; Mahmoud and Tantawi, 2003). After the yield point, necking begins to develop along the length of the specimen which occurs near the top or the bottom, and not near the center of the specimen, and this is observed across all the ageing intervals (Figures 5b-d). However, for GFRP composite, linear load-displacement response, until the load approaches the ultimate load (and failure). GFRP degradation can be observed by the change of the resin colour. Delamination of the glass fibres is the main cause of the specimen failure. Sharp cracks also initiated as the immersed time in acidic environment increased. By increasing the immersion time, the strength of the fibres decreased and the failure of the composite material obtained with less stress.

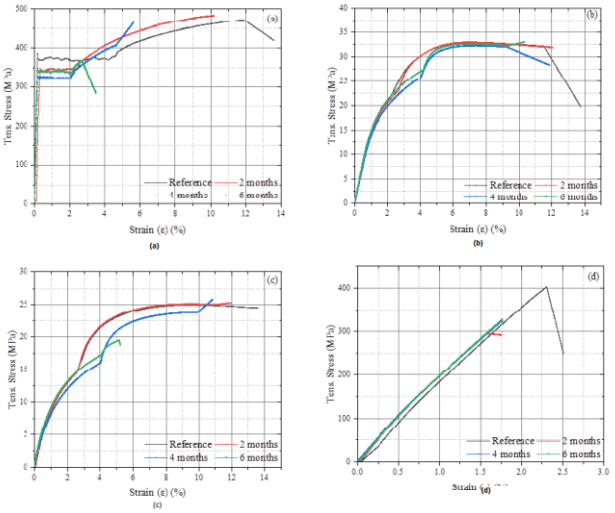

Figure 5. Tensile stress versus strain for **(a)** steel, **(b)** polypropylene, (c) polyethylene and **(d)** glass fiber reinforcement polymer.

The tensile strength, as well as moduli of the materials, are presented in Tables 2 and 3. Table 2 shows that the tensile strength of materials was slightly decreased during the first 2 months after soaking in the acid solution, and increased gradually afterwards. The tensile strength of steel and GFRP specimens will eventually decline to a very low level around 495 MPa and 342 MPa after 4 months of soaking in the acid solution at a constant temperature. It should be mentioned that metal failure is due to single propagation of the crack, compared with the additional failure of the GFRP. Defects and voids in the matrix, form macrocracks. During experimental procedure, moisture induced swelling of the matrix, which led to fibre-matrix debonding. Thus, swelling results in weakening the fibre-matrix adhesion and is instrumental in generating microcracks in the matrix

(Han and Nairn, 2003; Bergeret and Ienny, 2009; Haddar*et al.*, 2014; Karger-Kocsis, 1991; Kawaia *et al.*, 2017; Barbouchi *et al.*, 2007; Sindhu *et al.*, 2007; Kim and Youn, 2007; Postawa and Kwiatkowski, 2006; Chen *et al.*, 2000; Zhou and Li, 2005; Pons *et al.*, 2011). As the immersion time increased, the tensile strength of GFRP decreased more than 24% after ageing (Table 1 and Figure 5).

Generally, direct immersion of the polymer and polymer composites in acidic solutions resulted in the degradation of the mechanical properties over a relatively limited time (Haddar*et al.*, 2014; Karger-Kocsis, 1991; Kawaia *et al.*, 2017; Barbouchi *et al.*, 2007; Sindhu *et al.*, 2007; Kim and Youn, 2007; Postawa and Kwiatkowski, 2006; Chen *et al.*, 2000). Furthermore, from Table 1, no further degradation in the tensile strength of the thermoplastic materials (PE, PP) after 4 months of soaking in the acidic solution. This is one reason why thermoplastic polymer matrices are suitable for biogas applications (Mahmoud and Tantawi, 2003). Generally, thermoplastic materials swelling capacity depends on the structure which is determined by the method and conditions of specimen preparation (Pons *et al.*, 2011; Bowden and Young, 1974; Detrez and Roland, 2008; Drozdov and Christiansen, 2003; Mahmoud and Tantawi, 2003).

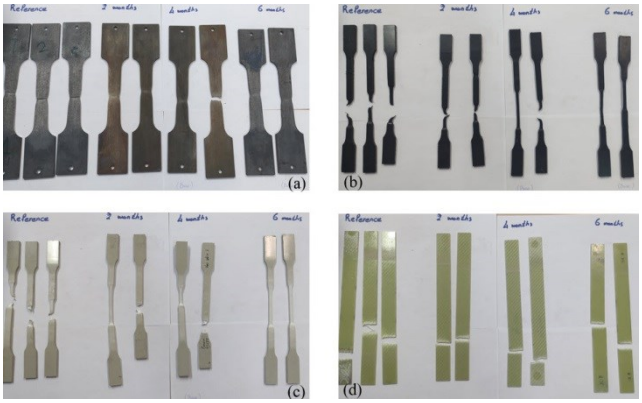

Figure 6. Tensile test failure modes for (a) steel, (b) polyethylene, (c) polypropylene and (d) glass fiber reinforced polymer.

Table 1. Summary of tensile test results.

Months	Tensile Strength [MPa]							
	St-37		PE-100		PP		GFRP	
	Avg. values	Std. Dev.	Avg. values	Std. Dev.	Avg. values	Std. Dev.	Avg. values	Std. Dev.
0	493.5	1.5	25.6	0.07	33.0	0.30	406.1	22.82
2	491.6	2.6	25.7	0.30	33.5	0.18	310.7	22.14
4	499.4	2.7	24.0	0.54	32.3	0.29	324.5	21.80
6	496.9	1.5	23.4	0.14	32.6	0.59	325.0	22.25

Table 2. Summary of Youngs' modulus results.

Months	Young ‘s Modulus [MPa]							
	St-37		PE-100		PP		GFRP	
	Avg. values	Std. Dev.	Avg. values	Std. Dev.	Avg. values	Std. Dev.	Avg. values	Std. Dev.
0	209.60	4.4	1.38	0.189	1.76	0.014	22.82	0.13
2	235.00	6.8	1.27	0.018	1.79	0.041	22.49	0.02
4	196.70	6.5	1.15	0.025	1.68	0.065	21.80	0.11
6	194.70	5.2	1.17	0.0	1.79	0.011	22.25	0.29

Table 3. Comparison of Finite Element (F) and Experimental results (X).

Months	Tensile Strength [MPa]							
	St-37		PE		PP		GFRP	
	X	F	X	F	X	F	X	F
0	493.5	491.35	25.6	26.36	33.0	34.93	406.1	415.15
2	498.7	483.33	25.9	26.12	33.7	35.07	348.4	362.12
4	480.1	396.73	23.8	24.49	32.3	33.75	344.5	353.16
6	495.7	401.66	23.8	24.36	32.1	30.06	304.8	323.71

Table 2 shows the Young’s modulus as a function of the treatment time in acidic solution at a stable temperature. Compared with the reduction in the tensile strength, the decrease in the elastic modulus was less pronounced. Furthermore, Table 3 reveals only small variations in the elastic modulus after ageing except for GFRP with a maximum loss of 17.94%.

3.3. Finite element modelling and results

Implicit finite element simulations of the tensile test were carried out using Abaqus. The dimensions of the specimens were presented in a previous section (Figure 1). Two different models were used to model the specimens. First, an elastic-perfectly plastic model was used for the polymers and metallic materials. By using such model, a progressive ductile failure can be predicted. Furthermore, for GFRP specimens a linear elastic behaviour was selected. Two different elements are also used. More than 20000 linear eight-node elements (C3D8R) and four-node elements (S4R) were used for metal (and thermoplastic materials) and polymer composite, respectively. The models were analyzed according to the boundary conditions shown in Figure 7.

Figure 7. Typical finite element mesh and loading and boundary conditions of the specimens.

The displacement was applied incrementally, to avoid the possibility of convergence to an incorrect solution. The theory of damage mechanics (damage initiation criterion and damage evolution law) was used, which takes into account the to predict the damage caused by nucleation, growth, and aggregation of voids. Using this theory, it can be predicted the necking instability (damage initiation criterion), as well as the rate of degradation of the material stiffness (damage evolution law). The finite element results are depending on the element mesh size. Table 3 summarizes both the finite element results and the experimental results. The numerical findings are directly in line with the experimental findings (Figure 7).

4. Conclusions

The objective of this study was to understand the durability of four different materials exposed to an acidic environment. The experimental results reveal swelling that leads to a decrease in mechanical properties. By increasing the immersed time from 0 to 6 months, the tensile strength slightly increases. However, mechanical properties decreased as the immersed time increased. For steel specimens, the experimental procedure shows that failure is estimated in terms of propagation of a single crack, while the failure of GFRP may be caused because of multiple microcracks (defects and voids) in the matrix. Thermoplastic materials (PP, PE) could be alternative solutions for biogas applications.

Acknowledgements

This research has been co-financed by the European Union and Greek national funds through the Operational Program Competitiveness, Entrepreneurship and Innovation, under the call RESEARCH–CREATE–INNOVATE (project code: T1EDK-00471).

References

Al-Salloum Y.A., El-Gamal S., Almusallam T.H., Alsayed S.H. and Aqel M. (2013). Effect of harsh environmental conditions on the tensile properties of GFRP bars. *Composites Part B: Engineering,* **45**(1), 835–44.

Azuma Y., Takeda H., Watanabe S. and Nakatani H. (2009). Outdoor and accelerated weathering tests for polypropylene and polypropylene/talc composites: A comparative study of their weathering behaviour. *Polymer Degradation and Stability*, **94**, 2267–2274.

Barbouchi S., Bellenger V., Tcharkhtchi A., Castaing P. and Jollivet T. (2007). Effect of water on the fatigue behaviour of a pa66/glass fibers composite material. *Journal of materials science*, **42**, 2181–2188.

Bentiss F., Lagrenee M. and Traisnel M. (2000). 2,5-Bis(n-Pyridyl)-1,3,4-Oxadiazoles as Corrosion Inhibitors for Mild Steel in Acidic Media Corrosion, **56**, 733–742.

Bergeret A., Ferry L. and Ienny P. (2009). Influence of the fibre/matrix interface on ageing mechanisms of glass fibre reinforced thermoplastic composites (PA-6,6, PET, PBT) in a hygrothermal environment. *Polymer Degradation and Stability*, **94**, 1315–1324.

Bowden P.B. and Young R.J. (1974). Deformation mechanisms in crystalline polymers. *Journal of Materials Science*, **9**, 2034–2051. https://doi.org/10.1007/bf00540553.

Chen X., Lam Y.C.C. and Li D.Q.Q., *Journal of Mechanical Working Technology,* 2000, **101**, 275–280.

Chen Y., Davalos J.F., Ray I. and Kim H.Y. (2007). Accelerated aging tests for evaluations of durability performance of FRP reinforcing bars for concrete structures. *Composite Structures,* **78**(1), 101–11.

Detrez F. and Roland S. (2008). Nano-Scale Deformation Mechanisms in Semi-Crystallin Polymers: In Situ Atomic Force Microscopy Study and Modeling. Université Lille I.

Diamantis V., Eftaxias A., Stamatelatou K., Noutsopoulos C., Vlachokostas C., Aivasidis A. (2021). Bioenergy in the era of circular economy: anaerobic digestion technological solution to produce biogas from lipid-rich wastes. *Renewable Energy* **168**, 438–447.

Drozdov A.D. and Christiansen J.D. (2003). Nonlinear time-dependent response of isotactic polypropylene. *Journal of Rheology*. (N.Y.N.Y), **47**, 595–618. 10.1122/1.1567753

Durnie W. and De Marco R. (199). A Jefferson ; B Kinsella, Development of a Structure – Activity Relationship for Oil Field Corrosion Inhibitors. *Journal of the Electrochemical Society*, **146**, 1751–1756.

EU Regulation. (2019/1009)of the European Parliament and of the Council of 5 June 2019 laying down rules on the making available on the market of EU fertilising products and amending Regulations (EC) No 1069/2009 and (EC) No 1107/2009 and repealing Regulation (EC) No 2003/2003.

Georgiou D., Liliopoulos V and Aivasidis A. (2019). Investigation of an integrated treatment technique for anaerobically digested animal manure: Lime reaction and settling, ammonia stripping and neutralization by biogas scrubbing. *Bioresource Technology Reports,* **5**, 127–133.

Haddar N., Ksouri I., Kallel T. and Mnif N. (2014). Effect of Hygrothermal Ageing on the Monotonic and Cyclic Loading of Glass Fiber Reinforced Polyamide. *Polymer Composites*, **35**, 501–508.

Han M.H. and Nairn J.A. (2003). Hygrothermal ageing of polyimide matrix composite laminates. *Composites Part A: Applied science and manufacturing,* **34**, 979–986.

Karger-Kocsis J. (1991). Environmental stress corrosion behaviour of polyamides and their composites with short glass fiber and glass swirl mat. *Polymer bulletin*, **26**, 123–130.

Kawaia M., Takeuchia H., Taketa I., Tsuchiya A. (2017). Effects of temperature and stress ratio on fatigue life of injection molded short carbon fiber-reinforced polyamide composite. *Composites Part A: Applied Science and Manufacturing*, **98**, 9–24.

Kim C.H. and Youn J.R. (2007). Polym. Test, **26**, 862–868.

Landolt D. (1993). Corrosion et Chimie de Surfaces des MétauxPresse Polytechniques et Universitaire Ramandes, **12**, 20–100.

Liao K., Schultheisz C.R. and Hunston D.L. (1999). Effects of environmental aging on the properties of pultruded GFRP. *Composites Part B: Engineering*, **30**(5), 485–93.

Mahmoud M.K. and Tantawi S. (2003). Effect of strong acids on mechanical properties of glass/polyester GRP pipe at normal and high temperatures. *Polymer-Plastics Technology and Engineering*, **42**(4), 677–88.

Mano J.F., Sousa R.A., Reis R.L., Cunha A.M. and Bevis M.J. (2001). Viscoelastic behaviour and time–temperature correspondence of HDPE with varying levels of process-induced orientation. *Polymer*, **42**(14), 6187–98.

Matassa S., Pelagalli V., Papirio S., Zamalloa C., Verstraete W., Esposito G., Pirozzi F. (2022) Direct nitrogen stripping and upcycling from anaerobic digestate during conversion of cheese whey into single cell protein. *Bioresource Technology,* **358**, 127308.

Miao J., Yuan J.T., Han Y., Xu X.Q., Li L. and Wang K. (2018). Corrosion behavior of P110 tubing steel in the CO2-saturated simulated oilfield formation water with element sulfur addition. *Rare Metal Materials and Engineering,* **47**(7), 1965–72.

Pons N., Bergeret A., Benezet J.C., Ferry L. and Fesquet F. (2011). Polym. Test, **30**, 310–317.

Postawa P. and Kwiatkowski D. (2006). J Achiev. Mater. Manuf Eng, **18**, 171–174.

Qi D.T., Li H.B., Cai X.H., Zhang S.H. and Yan M.L. (2011). Application and qualification of reinforced thermoplastic pipes in chinese oilfields. Beijing: ICPTT.

Roberge P.R. (2008). Corrosion Engineering: Principles and Practice, McGraw-Hill Professional., **1**, 484.

Robert M. and Benmokrane B. (2013). Combined effects of saline solution and moist concrete on long-term durability of GFRP reinforcing bars. *Construction and Building Materials,* **38**, 274–84.

Samimi A. and Zarinabadi S. (2012). Application Polyurethane as Coating in Oil and Gas Pipelines. *International Journal of science and investigations*. Investig, **1**, 43–45.

Samimi A. and Zarinabadi V. (2011). Scrutiny Water Penetration in Three-layer Polyethylene Coverage. *Journal of American science*, **7**(1), 1032–1036.

Sastri V.S. (1998). Corrosion Inhibitors: Principles and Applications. John Wiley and Sons, Chichester, UK.

Sindhu K., Joseph K., Joseph J.M. and Mathew T.V. (2007). Degradation studies of coir fiber/polyester and glass fiber/polyester composites under different conditions. *Journal of Reinforced Plastics and Composites*, **26,** 1571–1585.

Spyridonidis A., Vasiliadou I.A., Stamatelatou K. (2022). Effect of zeolite on the methane production from chicken manure.*Sustainability,* **14**, 2207.

Tallman D.E., Pae Y. and Bierwagen G.P. (1999). Conducting Polymers and Corrosion: Polyaniline on Steel. *Corrosion*, **55**, 779–786.

Zhou H. and Li D. (2005). Residual stress analysis of the post-filling stage in injection moulding. *International Journal of Advanced Design and Manufacturing Technology*, **25**, 700–704.